

Supporting Information

Semiconducting SN₂ Monolayer with Three-Dimensional Auxetic Properties: A Global Minimum with Tetracoordinated Sulfurs

Fengyu Li,^{a,#*} Xiaodong Lv,^{a,#} Jinxing Gu,^b Kaixiong Tu,^b Jian Gong,^a Peng Jin,^{c,*}

Zhongfang Chen^{b,*}

^a *School of Physical Science and Technology, Inner Mongolia University, Hohhot, 010021, China*

^b *Department of Chemistry, The Institute for Functional Nanomaterials, University of Puerto Rico, Rio Piedras Campus, San Juan, PR 00931, USA*

^c *School of Materials Science and Engineering, Hebei University of Technology, Tianjin 300130, China.*

*Corresponding Author: fengyuli@imu.edu.cn (FL); china.peng.jin@gmail.com (PJ); zhongfangchen@gmail.com (ZC)

Equal contribution to this work.

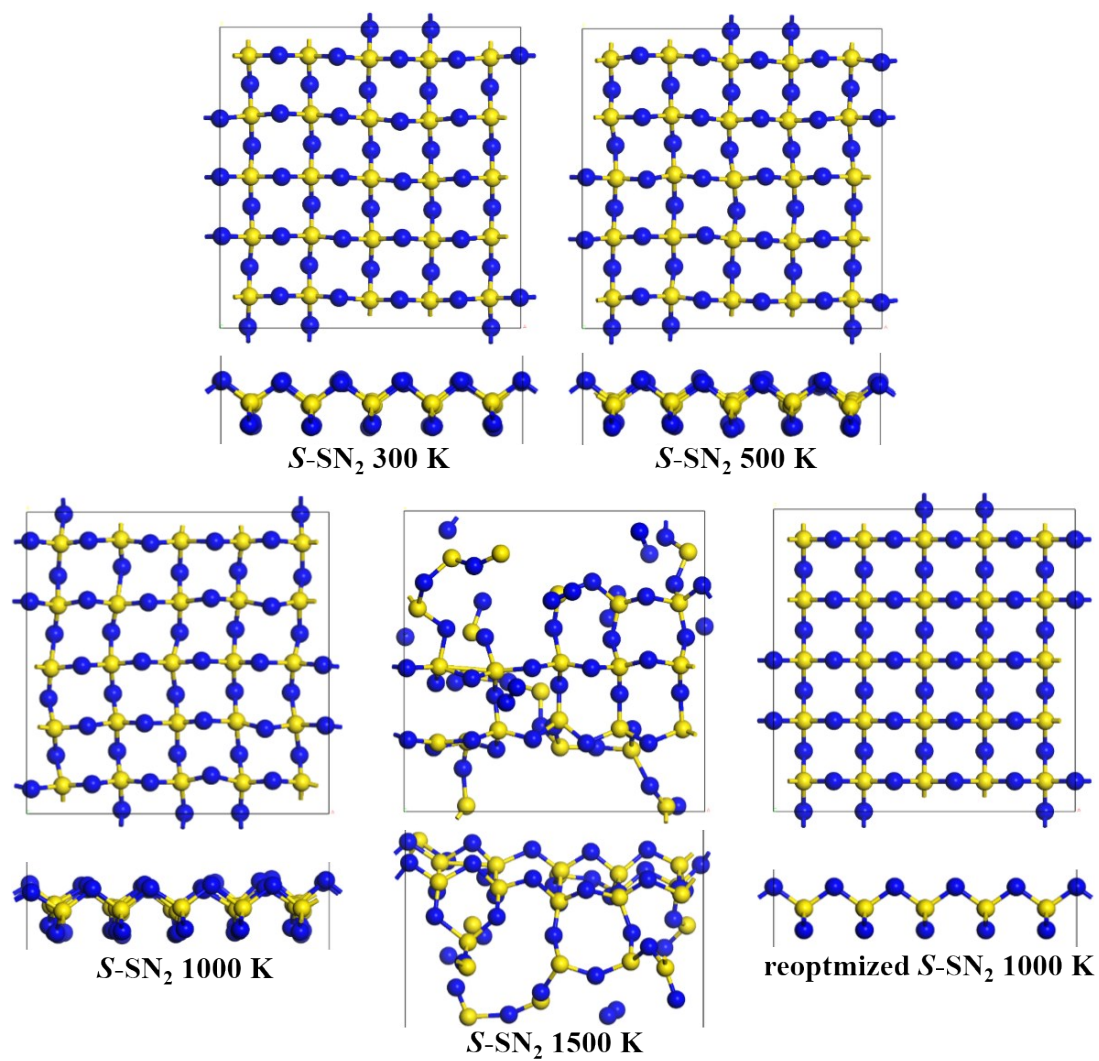


Fig. S1. The snapshots (top and side views) of the $S-SN_2$ monolayer after 10 ps FPMD simulations at 300 K, 500 K, 1000 K, and 1500 K, and the reoptimized structure of the final structure of $S-SN_2$ monolayer after 10 ps MD simulation at 1000 K.

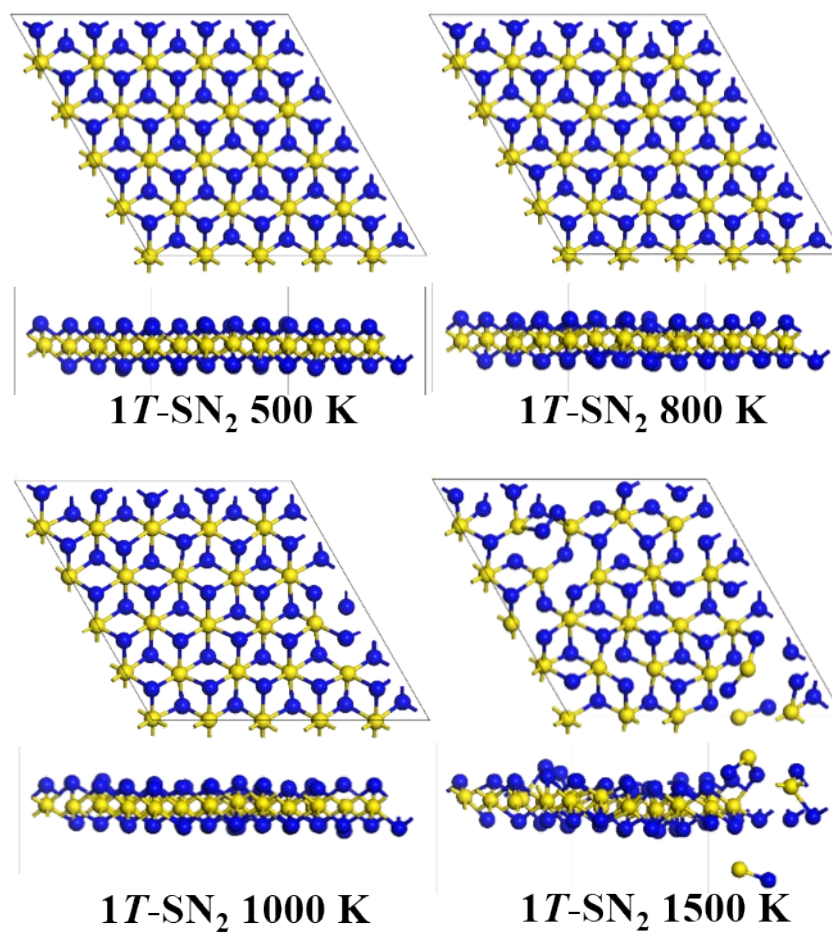


Fig. S2. The snapshots (top and side views) of the 1T-SN₂ monolayer after 10 ps FPMD simulations at 500 K, 800 K, 1000 K, and 1500 K.

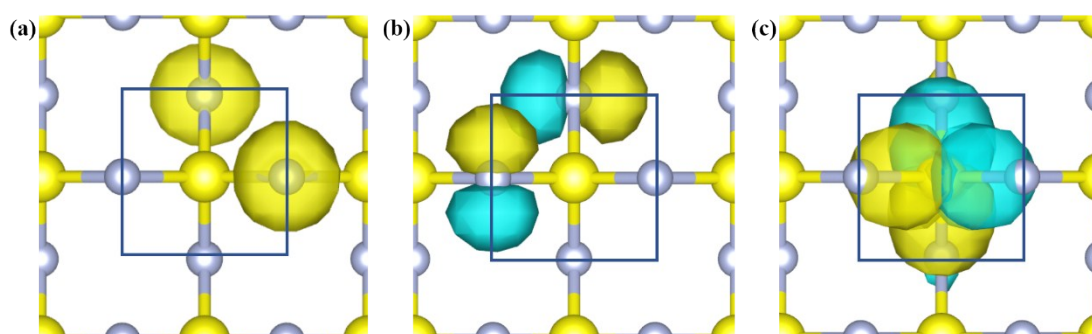


Fig. S3. The SSAdNDP chemical bonding pattern of the S-SN₂ unitcell (isovalue = 0.1 eÅ⁻³). Totally eight bonding patterns are revealed, including (a) two *sp*-orbital lone-pairs on N atoms, with occupation numbers (ONs) as 1.82; (b) two *p*-orbital lone-pairs on N atoms, with ONs as 1.75; (c) four two-center-two-electron chemical bonds between N and S atoms, with ONs as 1.97.

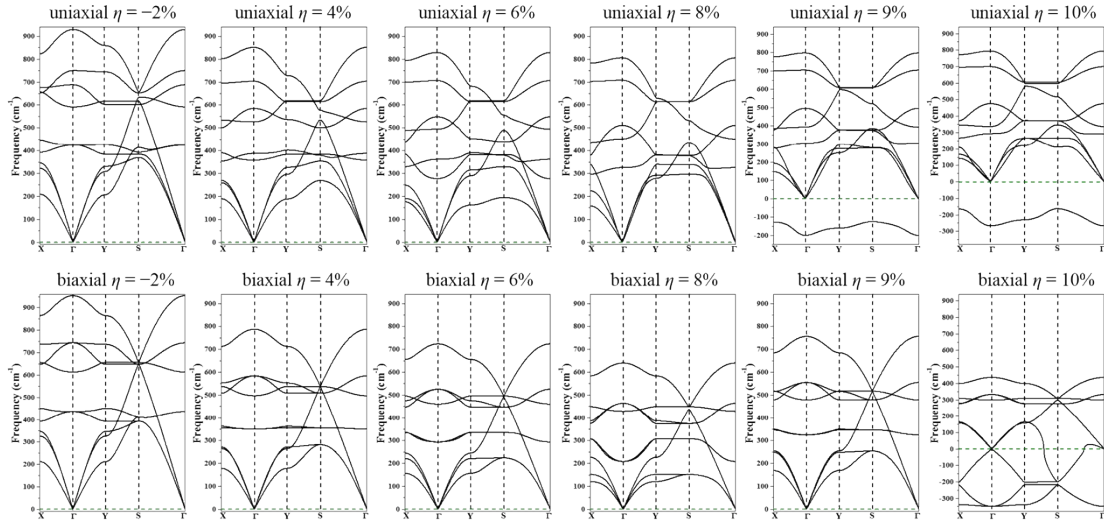


Fig. S4. The calculated phonon spectra of the $S\text{-SN}_2$ monolayer under uniaxial and biaxial strains.

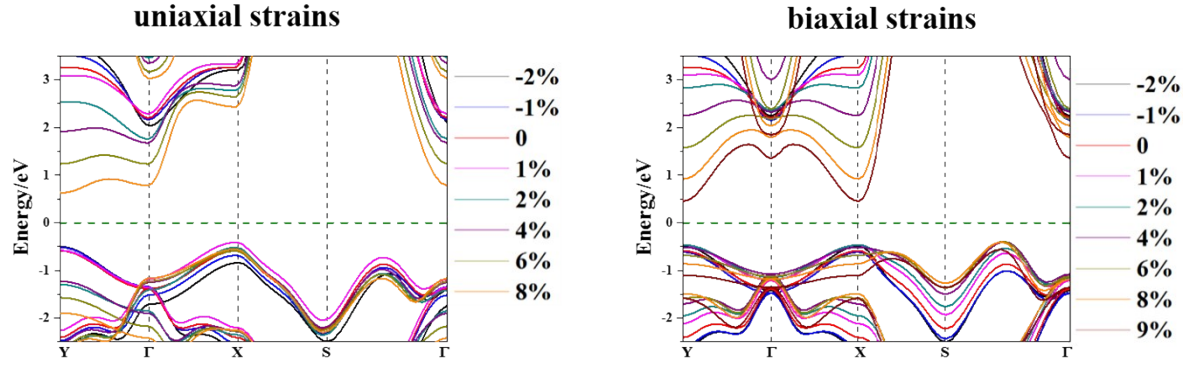


Fig. S5. The HSE06 band structures of the $S\text{-SN}_2$ monolayer under uniaxial and biaxial strains.

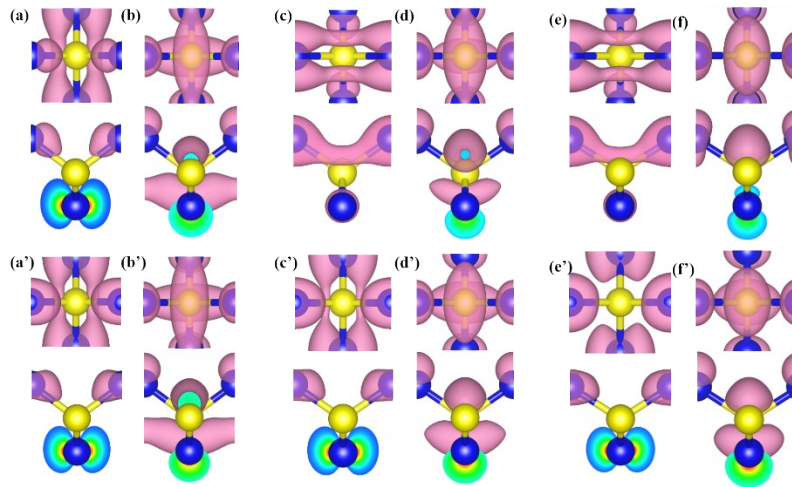


Fig. S6. The spatial distributions of wave functions of VBM and CBM from the top and side views (isovalue: $0.02 e\text{\AA}^{-3}$) for the $S\text{-N}_2\text{S}$ monolayer under uniaxial strain of -2% (a,b), 2% (c,d) and 6% (e,f), as well as biaxial strain of -2% (a',b'), 2% (c',d') and 6% (e',f').

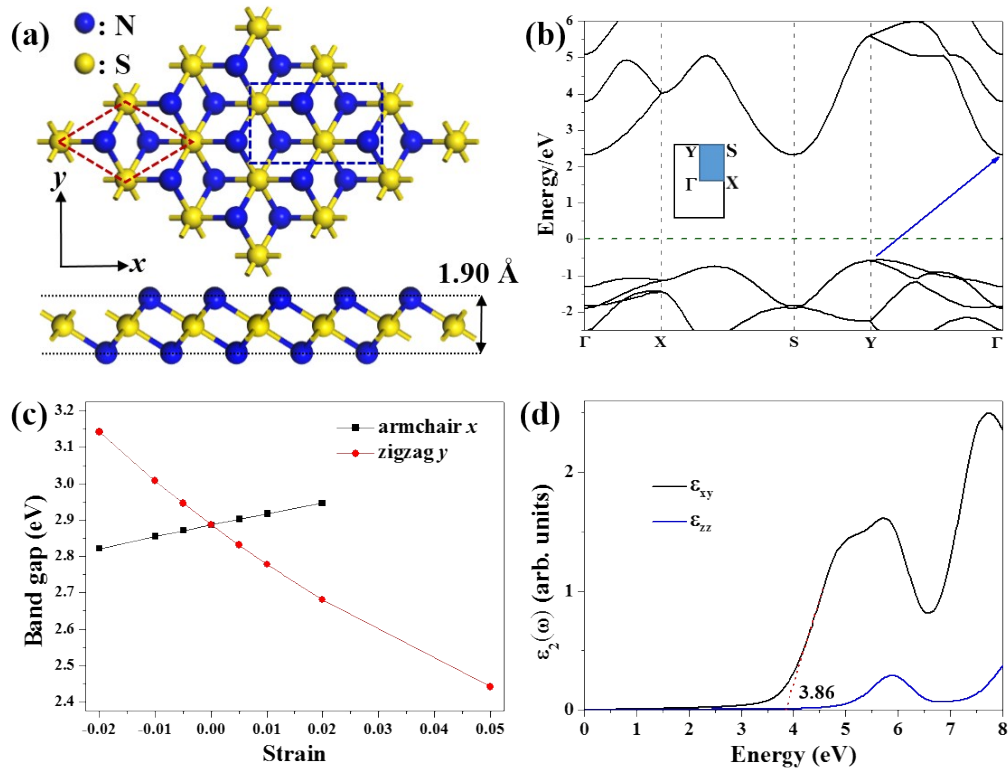


Fig. S7. 1T-SN₂ monolayer: (a) Structure from top and side views (a 3×3×1 supercell, the hexagonal unitcell and the orthogonal lattice are highlighte by the red dashed diamond and the blue dashed rectangle, respectively); (b) band structure (the green dashed line denotes the Fermi level); (c) the HSE06 band gap of 1T-SN₂ monolayer as a function of the external strains along the x (armchair) and y (zigzag) uniaxial directions; (d) the computed imaginary dielectric constants of the 1T-SN₂ monolayer. The red dashed line denotes an approximate linear fitting for estimating the band edge of the first adsorption peak.

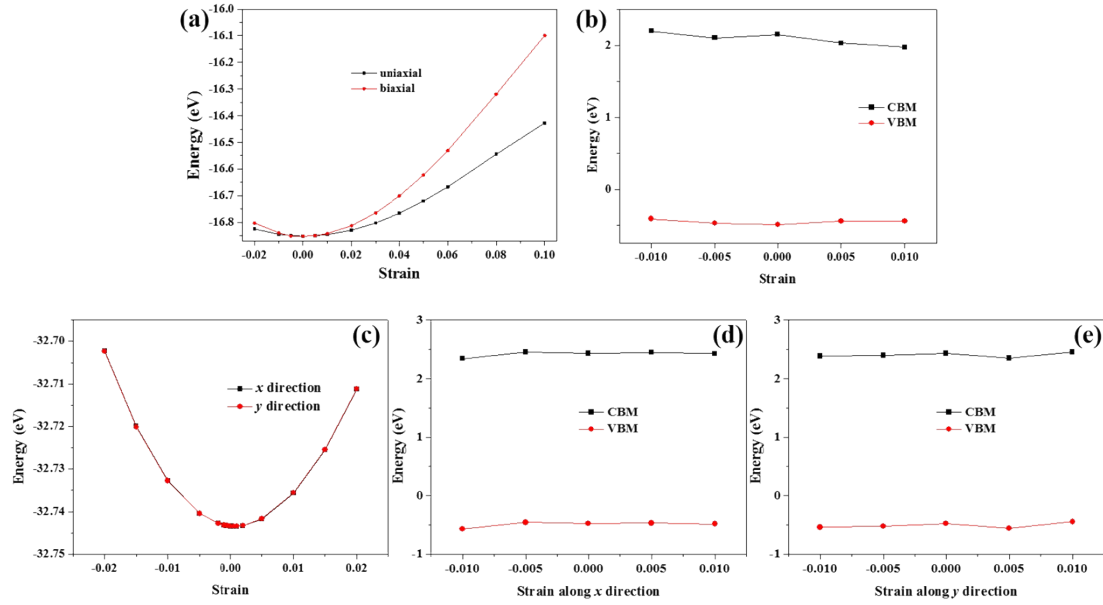


Fig. S8. The S - SN_2 monolayer (a,b): (a) The relationship between the total energy and uniaxial/biaxial strain of S - SN_2 ; (b) the HSE06 energy of VBM and CBM shift with respect to the lattice dilation and compression along x (y) direction. The $1T$ - SN_2 monolayer (c-e): The relationship between the total energy and strain along armchair (x) and zigzag (y) directions (c). The HSE06 energy of VBM and CBM shift with respect to the lattice dilation and compression along (d) armchair and (e) zigzag directions.

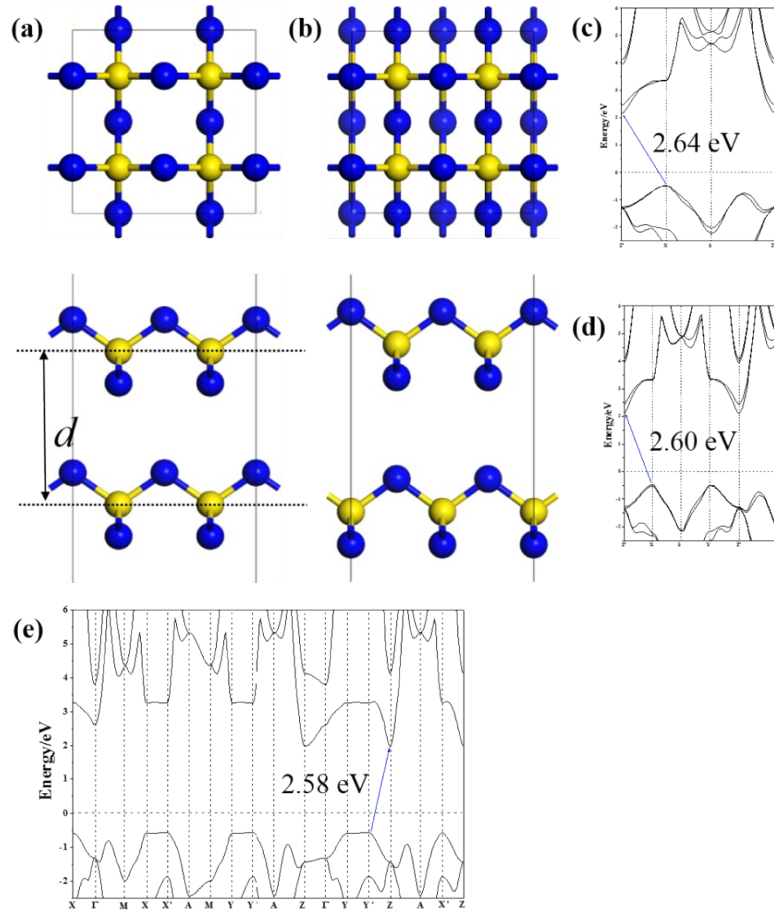


Fig. S9. The AA (a) and AB (b) stacking configurations for $S\text{-SN}_2$ bilayer from both the top and side views (a 2×2 supercell of the hexagonal lattice). Band structures of the $S\text{-SN}_2$ bilayer in AA (c) and AB (d) stacking configurations, as well as the bulk (e).

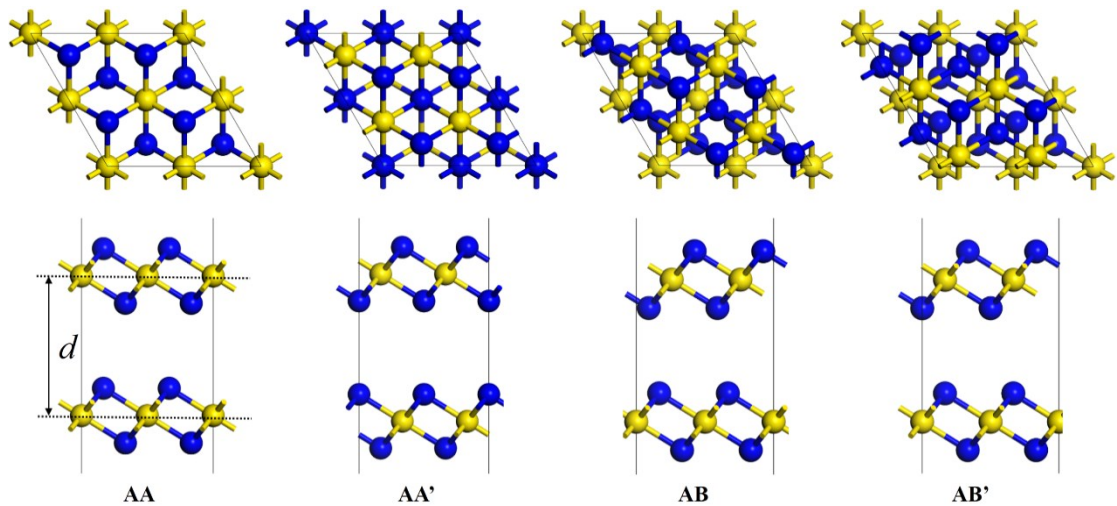


Fig. S10. Different stacking configurations for $1T\text{-SN}_2$ bilayer from both the top and side views (a 2×2 supercell of the hexagonal lattice). The interlayer distance (d) was labeled in the AA stacking.

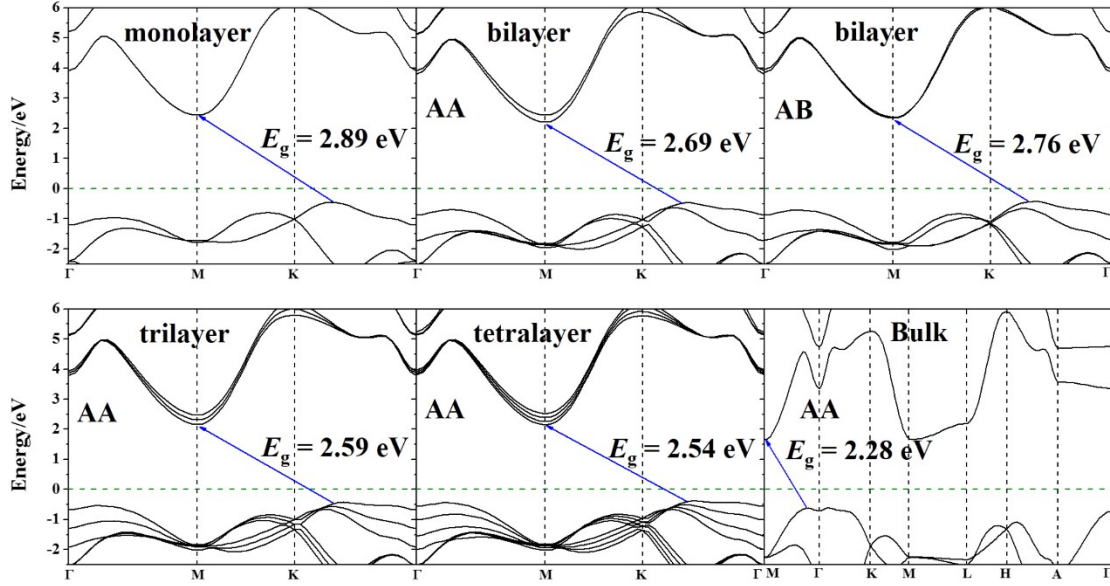


Fig. S11. Band structures of the few-layer and bulk SN_2 in 1T phase.

Table S1. The interlayer distance (d , in Å) and binding energy (E_b , in eV) of 1T- SN_2 bilayer in different stacking configurations and trilayer, tetralayer and bulk of AA stacking.^a

bilayer				
Stacking	AA	AA'	AB	AB'
d	2.95	2.97	2.97	3.07
E_b	0.28	0.28	0.29	0.28
AA stacking				
	bilayer	trilayer	tetralayer	bulk
d	2.95	2.94	2.91/2.94	2.84
E_b	0.28	0.30	0.31	0.31

^a The binding energy of trilayer, tetralayer and bulk in AA stacking was calculated by $E_b = (3 \times E_{\text{monolayer}} - E_{\text{trilayer}})/3$, $E_b = (4 \times E_{\text{monolayer}} - E_{\text{tetralayer}})/4$, and $E_b = E_{\text{monolayer}} - E_{\text{bulk}}$, respectively.